

Correlation-Based Approach to Color Image Compression

Evgeny Gershikov*, Emilia Lavi-Burlak and Moshe Porat

*Department of Electrical Engineering, Technion - Israel Institute of Technology,
Haifa 32000, Israel*

Abstract

Most coding techniques for color image compression employ a de-correlation approach - the RGB primaries are transformed into a de-correlated color space, such as YUV or YCbCr, then the de-correlated color components are encoded separately. Examples of this approach are the JPEG and JPEG2000 image compression standards. A different method, of a Correlation Based Approach (CBA) is presented in this paper. Instead of de-correlating the color primaries, we employ the existing inter-color correlation to approximate two of the components as a parametric function of the third one, called the base component. We then propose to encode the parameters of the approximation function and part of the approximation errors. We use the DCT (Discrete Cosine Transform) block transform to enhance the algorithm's performance. Thus the approximation of two of the color components based on the third color is performed for each DCT subband separately. We use the Rate-Distortion theory of subband transform coders to optimize the algorithm's bits allocation for each subband and to find the optimal color components transform to be applied prior to coding. This pre-processing stage is similar to the use of the RGB to YUV transform in JPEG and may further enhance the algorithm's performance. We introduce and compare two versions of the new algorithm and show that by using a Laplacian probability model for the DCT coefficients as well as down-sampling the subordinate colors, the compression results are further improved. Simulation results are provided showing that the new CBA algorithms are superior to presently available algorithms based on the common de-correlation approach, such as JPEG.

Key words: Color image compression, Inter-color correlation, Correlation Based Approach, DCT block transform, Rate-Distortion model, Color components transform, Optimal rates allocation

* Corresponding author. Tel.: +972-4-8294725; Fax: 972-4-8294799.
Email address: eugeny@tx.technion.ac.il (Evgeny Gershikov).

1 Introduction

Recently a new algorithm for color image compression was introduced by Goffman and Porat [8]. This algorithm utilizes the high inter-color correlations between RGB color components of natural images ([6], [8], [11], [14], [18], [22]) without transforming them into another color domain. It does so by dividing the image into square blocks, expanding two of the color primaries (the dependent colors) as a polynomial function of the third (base) color for each block. This way only the polynomial coefficients are encoded for each block of the dependent colors, whereas the base color component is encoded by any monochromatic compression technique. The choice of the base was examined in [8] with general tendency to choose the Green. The conclusion in [8] was that the new algorithm produces less color artifacts than the common de-correlation approach at high compression ratios. The de-correlation approach (such as JPEG [20] and JPEG2000 [10], [16]) consists of transforming the color components into a de-correlated color space, then separately encoding each of the obtained color components. This approach is the most common for color images, however, it is not necessarily the optimal one. Additional examples of this approach can be found in [12] and [21].

The algorithm by Goffman and Porat may be considered as an example of a Correlation-Based Approach (CBA) to color image compression. In this work we introduce two new algorithms based on this approach. We use the DCT block transform [17] to enhance the compression performance. Thus the expansion of the dependent colors is done for each DCT subband instead of for each image block. However, not only the expansion coefficients are coded, but also the approximation errors for part of the subbands. Since the DCT block transform is a special case of a subband transform, we propose to employ the recently developed Rate-Distortion theory for subband transform coders [4]. This theory allows us not only to find the optimal bits allocation for the subbands in MSE (Mean Square Error) sense, but also the optimal Color Components Transform (CCT) as an efficient pre-processing stage.

The structure of this paper is as follows. In Subsections 1.1, 1.2 and 1.3 we review the Rate-Distortion theory for subband transform coders and the algorithms for calculating the optimal subband rates and the corresponding PCM quantization steps. In Sections 2 and 3 we introduce two versions of the new algorithm and discuss how the Rate-Distortion theory is used in their optimization. Section 4 deals with optimizing the color components transform. Then in Section 5 down-sampling of the subordinate colors and use of the Laplacian probability model for the DCT coefficients are described. This model allows reduction of the algorithms' complexity and provides lower coding distortion for the same transmission rate. Another potential improvement of the algorithms' performance is presented in Section 6. Simulation results of the new algorithms and their comparison to JPEG as a representative of the de-correlation approach are discussed in Section 7. Finally, conclusions and

summary are given in Section 8.

1.1 Rate-Distortion theory of subband transform coders

In [4] a general subband transform coder for color images was considered, based on the following steps.

- Pre-processing: apply a CCT to the RGB color components of the given image. Denoting the RGB components in vector form as $\mathbf{x} = [R \ G \ B]^T$ and the new color components as $\tilde{\mathbf{x}} = [C1 \ C2 \ C3]^T$, this stage can be written as:

$$\tilde{\mathbf{x}} = \mathbf{M}\mathbf{x} \quad (1)$$

for some 3×3 CCT matrix \mathbf{M} .

- Apply a subband transform, such as DCT or DWT (Discrete Wavelet Tree) or any filter bank decomposition to each color component. The subband transform is usually assumed to be non-expansive, i.e., it transforms a signal of length N to a signal with the same length.
- Quantize the coefficients of each subband of each color component. A uniform scalar quantizer was considered. We refer to this stage as applying the PCM (Pulse Code Modulation) scheme.
- Post-processing: encode the quantized coefficients in a lossless manner, such as run-length coding, delta modulation or entropy coding.

At high rates R the Rate-Distortion behavior of the basic PCM scheme applied to a random signal x with variance σ_x^2 is [7], [19]

$$d(R) = \varepsilon^2 \sigma_x^2 2^{-2R}, \quad (2)$$

where ε^2 is a constant dependent upon the distribution of x . This is only an approximate behavior or model, however, based on (2) the R-D (Rate-Distortion) model of a general monochromatic subband coder with B subbands can be expressed as

$$d^{SC}(\{R_b\}) = \sum_{b=0}^{B-1} \eta_b G_b d_b(R_b) = \sum_{b=0}^{B-1} \eta_b G_b \sigma_b^2 \varepsilon^2 2^{-2R_b}. \quad (3)$$

Here $d_b(R_b)$ is the MSE of subband b ($b \in 0, 1, \dots, B-1$), σ_b^2 is its variance, G_b is its energy gain [19], R_b is the rate allocated to it, and η_b is its sample rate. The sample rate of a subband is equal to the relative part of the number of coefficients in it from the total number of samples in the subband transformed signal. For a uniform subband transform, such as the block DCT $\eta_b = \frac{1}{B}$. Consider now a color image. The coding algorithm described in the beginning of this section may be regarded as applying a CCT to the image, followed

by monochromatic subband coding of each of the new color components. The Rate-Distortion model of this algorithm is

$$d(\{R_{bi}\}, \mathbf{M}) = \frac{1}{3} \sum_{i=1}^3 \sum_{b=0}^{B-1} \eta_b G_b \sigma_{bi}^2 \varepsilon_i^2 e^{-aR_{bi}} \left((\mathbf{M}\mathbf{M}^T)^{-1} \right)_{ii}, \quad (4)$$

where $a = 2 \ln 2$ and σ_{bi}^2 and R_{bi} remain the same, but for subband b of color component i ($i \in 1, 2, 3$). Note that standard entropy coding is assumed here in the post-processing stage or alternatively this stage is not taken into account. Minimizing the expression of Equation (4) under the rate constraint

$$\sum_{i=1}^3 \sum_{b=0}^{B-1} \eta_b R_{bi} = R, \quad (5)$$

as well as non-negativity constraints for the rates lead to the optimal subband rates allocation. If we denote the set of non zero (or active) rates in the color component i by Act_i , i.e., $Act_i \triangleq \{b \in [0, B-1] \mid R_{bi} > 0\}$, then the active optimal rates are given by

$$R_{bi} = \frac{R}{\sum_{j=1}^3 \xi_j} + \frac{1}{a} \ln \left(\frac{\varepsilon_i^2 G_b \sigma_{bi}^2 \left((\mathbf{M}\mathbf{M}^T)^{-1} \right)_{ii}}{\prod_{k=1}^3 \left[\left(\varepsilon_k^2 G M A_k \left((\mathbf{M}\mathbf{M}^T)^{-1} \right)_{kk} \right)^{\frac{\xi_k}{\sum_{j=1}^3 \xi_j}} \right]} \right), \quad (6)$$

where

$$\xi_i \triangleq \sum_{b \in Act_i} \eta_b, \quad G M A_i \triangleq \prod_{b \in Act_i} (G_b \sigma_{bi}^2)^{\frac{\eta_b}{\xi_i}}. \quad (7)$$

The rate constraint of (5) and the optimal rates of (6) do not account for down-sampling of some of the color components as, for example, is done in JPEG [20]. To do so a down-sampling factor α_i is introduced for color component i , so that if the down-sampling is by a factor of 2 horizontally and vertically then:

$$\alpha_i = \begin{cases} 1 & \text{full component} \\ 0.25 & \text{down-sampled component.} \end{cases}$$

Thus the rate constraint becomes:

$$\sum_{i=1}^3 \alpha_i \sum_{b=0}^{B-1} \eta_b R_{bi} = R, \quad (8)$$

and the solution for the rates is:

$$R_{bi} = \frac{R}{\sum_{j=1}^3 \alpha_j \xi_j} + \frac{1}{a} \ln \left(\frac{\frac{\varepsilon_i^2 G_b \sigma_{bi}^2 ((\mathbf{M}\mathbf{M}^T)^{-1})_{ii}}{\alpha_i}}{\prod_{k=1}^3 \left(\frac{((\mathbf{M}\mathbf{M}^T)^{-1})_{kk} \varepsilon_k^2 GMA_k}{\alpha_k} \right)^{\frac{\alpha_k \xi_k}{\sum_{j=1}^3 \alpha_j \xi_j}}} \right) \quad (b \in Act_i). \quad (9)$$

There is still a question of how the active rates are determined. The iterative algorithm introduced in [4] for this purpose is described in the next subsection.

1.2 Determining the active subbands

The following algorithm can be used to find the active subbands iteratively:

- (1) Assume all the subbands are active and calculate the rates.
- (2) While some $R_{bi} < 0$
 - Set $Act_i = \{b \in [0, B - 1] \mid R_{bi} > 0\}$
 - Calculate new rates.
- (3) Check that the Lagrange multipliers $\mu_{bi} \geq 0$, where:

$$\mu_{bi} = \begin{cases} \frac{a}{3} \eta_b \left((\mathbf{M}\mathbf{M}^T)^{-1} \right)_{ii} \varepsilon_i^2 \left(G_0 \sigma_{0i}^2 e^{-aR_{0i}} - G_b \sigma_{bi}^2 \right) & b \notin Act_i \\ 0 & b \in Act_i \end{cases}.$$

Here σ_{0i}^2 and R_{0i} are the variance and rate, respectively, of subband 0 of component i . This subband can be any subband that can be assumed to be active always. Usually we would choose the subband with the maximal energy (variance) for that component, e.g., the DC subband for the DCT.

Once the optimal rates have been determined, there is still the question of the size of the PCM quantization steps to choose to achieve these rates. The quantization steps algorithm proposed in [1] is given next.

1.3 Determining the optimal PCM steps

The algorithm consists of the following stages:

- Calculate the optimal rates R_{bi}^* (using (6) or (9)).
- Set some initial quantization steps Δ_{bi} and calculate the resulting rates R_{bi} .
The rate R_{bi} is the entropy of subband b of color component i .
- Update the quantization steps according to:

$$\Delta_{bi}^{new} = \Delta_{bi} 2^{-(R_{bi}^* - R_{bi})}$$

until the optimal rates R_{bi}^* are sufficiently close, i.e., $E(|R_{bi}^* - R_{bi}|) < \varepsilon$ for some small constant ε . $E()$ stands here for statistical mean.

This algorithm provides a means of how to deal with the active subbands. The coefficients of the non-active subbands are zeroed.

2 The basic CBA algorithm

We begin this section with the introduction of the basic framework for the CBA algorithms. Given a color image in the RGB domain denoted $\mathbf{x} = [R \ G \ B]^T$ at each pixel, we first apply a CCT to the color components to obtain $\tilde{\mathbf{x}} = [C1 \ C2 \ C3]^T = \mathbf{M}\mathbf{x}$ as in Equation (1). This stage is optional, i.e., the C1, C2, C3 components can be simply the original R, G, B (possibly with some order change). Then we apply the DCT block transform on each of the new color components and group the DCT coefficients into B subbands. For example, for a DCT block size of 8×8 , $B = 64$. We denote the subband b , ($b \in \{0, 1, \dots, B - 1\}$) coefficients of the color component i by y_{bi} . Now without loss of generality we approximate C2 and C3 in each subband as a function of C1. In [8] Goffman and Porat suggested to use linear approximation for the dependent colors in each image block. The motivation for this is that the color components in the image domain are highly correlated in a small neighborhood whereas high correlations suggest a linear dependency. The same is true, however, for the DCT subbands - the inter-color correlations are high. Thus we suggest approximating C2 and C3 in subband b according to:

$$\begin{aligned}\hat{y}_{b2} &= \tau_{b1} \cdot y_{b1} + \tau_{b0} \\ \hat{y}_{b3} &= \beta_{b1} \cdot y_{b1} + \beta_{b0},\end{aligned}\tag{10}$$

for some constant expansion coefficients $\tau_{b0}, \tau_{b1}, \beta_{b0}, \beta_{b1}$. We use the least squares (LS) or MSE criterion to find these coefficients, i.e., we look for τ_{b0}, τ_{b1} minimizing

$$E[(y_{b2} - \hat{y}_{b2})^2] = E[(y_{b2} - \tau_{b1} \cdot y_{b1} - \tau_{b0})^2]\tag{11}$$

and the same for β_{b0}, β_{b1} with y_{b3} replacing y_{b2} and β replacing τ . Equation (11) can be rewritten as:

$$E[(y_{b2} - \hat{y}_{b2})^2] = \text{var}(y_{b2} - \tau_{b1} \cdot y_{b1}) + E^2[(y_{b2} - \tau_{b1} \cdot y_{b1} - \tau_{b0})],\tag{12}$$

where $\text{var}()$ stands for variance. Thus τ_{b1} only minimizes the variance of the approximation error $e_{b2} \triangleq y_{b2} - \hat{y}_{b2}$, and τ_{b0} will have to be chosen to bring the error mean $E(e_{b2}) = E(y_{b2} - \tau_{b1} \cdot y_{b1} - \tau_{b0})$ to zero. The optimal coefficients

are thus:

$$\begin{aligned}\tau_{b1} &= \frac{\text{cov}(y_{b1}, y_{b2})}{\text{var}(y_{b1})} \\ \tau_{b0} &= E(y_{b2} - \tau_{b1} \cdot y_{b1}) = E(y_{b2}) - \frac{\text{cov}(y_{b1}, y_{b2})}{\text{var}(y_{b1})} \cdot E(y_{b1}),\end{aligned}\tag{13}$$

and similarly:

$$\begin{aligned}\beta_{b1} &= \frac{\text{cov}(y_{b1}, y_{b3})}{\text{var}(y_{b1})} \\ \beta_{b0} &= E(y_{b3} - \beta_{b1} \cdot y_{b1}) = E(y_{b3}) - \frac{\text{cov}(y_{b1}, y_{b3})}{\text{var}(y_{b1})} \cdot E(y_{b1}).\end{aligned}\tag{14}$$

Here $\text{cov}()$ stands for covariance. The meaning of Equation (13) for τ_{b1} is that

$$\tau_{b1} = \frac{\sum_k E \left[\left(y_{b1}^k - E(y_{b1}) \right) \left(y_{b2}^k - E(y_{b2}) \right) \right]}{\sum_k E \left[\left(y_{b1}^k - E(y_{b1}) \right)^2 \right]},\tag{15}$$

where k is an index running on all the subband b coefficients, y_{b1}^k , for example, is the k^{th} coefficient for C1 and $E(y_{b1})$ is the mean value of the subband b coefficients for C1.

2.1 How good is the LS approximation of C2 and C3?

The MSE of C2 or C3 can be expressed as:

$$d_{Ci} = \frac{1}{B} \sum_{b=0}^{B-1} d_{bi}, \quad (i = 2, 3).\tag{16}$$

This expression, in fact, is the same as used in Equation (3) with energy gains $G_b = 1$ due to the orthogonality of the DCT and $\eta_b = \frac{1}{B}$ due to its uniformity. Similarly, d_{bi} denotes here the MSE of the subband b of the color component i . If we denote the correlation coefficient of C1 and C2 and the correlation coefficient of C1 and C3 in subband b by ρ_{b12} and ρ_{b13} , respectively, then using the coefficients of (13) and (14) results in the MSE distortions:

$$d_{bi} = \text{var}(y_{bi}) \left(1 - \rho_{b1i}^2 \right), \quad (i = 2, 3).\tag{17}$$

Thus, the greater the inter-color correlations in subband b is, the smaller the MSE of this subband becomes for approximated DCT coefficients with the same variance.

It is well known that the DCT concentrates most of the image energy in the DC

and low frequency subbands, thus greatly increasing their variances relative to the other subbands. It turns out that simply performing LS approximation for these subbands of C2 and C3 results in too large MSE distortions since the correlations ρ_{b1i} in (17) have to be very high (e.g., above 0.95) to provide for reasonable distortion. This is not the case in general and thus we suggest coding the approximation errors in addition to the expansion coefficients for the subbands with high variances. How exactly these subbands are chosen as well as how the errors are compressed is the subject of Subsection 2.3. Note that the d_{bi} of (17) is also the variance of the approximation error of the subband due to the effect of the zero order expansion coefficient τ_{b0} or β_{b0} that zeroes the error's mean value. Thus

$$\text{var}(e_{bi}) = \text{var}(y_{bi} - \hat{y}_{bi}) = \text{var}(y_{bi}) (1 - \rho_{b1i}^2), \quad (i = 2, 3). \quad (18)$$

Next we discuss the encoding of the expansion coefficients.

2.2 Coding the expansion coefficients

We suggest to use PCM with a uniform scalar quantizer (and different step size) for each of the coefficients. It turns out that a small number of bits can be allocated to each coefficient, e.g., 2 bits to the τ_{b0} and β_{b0} coefficients and 3 bits to τ_{b1} and β_{b1} . There is still correlation between the same coefficients of different subbands and thus one can employ delta modulation, for example, then entropy coding in the post-quantization stage. However, with such a small bits budget allocated to the coefficients, basic quantization should be sufficient.

The dynamic range of the coefficients is not predefined. Thus we employ two thresholds with any coefficient above the upper threshold or below the lower threshold being forced by the value of the corresponding threshold. Assuming that the coefficient being encoded (one of τ_{b0} , β_{b0} , τ_{b1} and β_{b1}) has mean μ and standard deviation σ , the lower and upper thresholds are chosen to be $\mu - K\sigma$ and $\mu + K\sigma$, respectively. K is a constant that can be chosen to be $K = 8$ as in [9].

2.3 Coding the approximation errors

The approximation errors have been defined above as, for example, $e_{b2} \triangleq y_{b2} - \tau_{b1} \cdot y_{b1} - \tau_{b0}$ for C2. We have, however, to introduce a correction here: the expansion coefficients used eventually in the calculation of these errors are the coefficients after quantization and reconstruction (i.e., $\hat{\tau}_{b1}$ instead of τ_{b1}).

Thus the errors to be coded are:

$$\begin{aligned}\hat{e}_{b2} &\triangleq y_{b2} - \hat{\tau}_{b1} \cdot y_{b1} - \hat{\tau}_{b0} \\ \hat{e}_{b3} &\triangleq y_{b3} - \hat{\beta}_{b1} \cdot y_{b1} - \hat{\beta}_{b0}.\end{aligned}\tag{19}$$

We propose to code the approximation errors using a uniform scalar quantizer for each subband. Then for each subband of C2 or C3, the MSE distortion will be actually a quantization error. As a result, we are able to use the theory mentioned in Subsection 1.1. The theoretical variances of the subbands, when the optimal expansion coefficients are used without quantization, are equal to the MSE distortions of Equation (17). Clearly, the quantization of the coefficients will increase the MSE distortions and generally the variances as well, however, substituting the real error variances σ_{bi}^2 in (6), the optimal subband rates can be calculated. The determination of the active subbands as well as the PCM steps for them is performed according to Subsections 1.2 and 1.3. Note that for non-active subbands only the expansion coefficients are sent and the approximation errors are all regarded as zero. Thus for these subbands the MSE distortions are due to the LS approximation and the PCM errors in the expansion coefficients themselves. In fact, due to the lack of correlation between the LS errors $y_{bi} - \hat{y}_{bi}$ and the PCM errors $e_{bi} - \hat{e}_{bi}$ the total MSE distortion for each non-active subband is the sum of the MSE errors of the two stages. As for the active subbands, the LS approximation only determines the variance of the coded error there whereas the subband MSE is equal to the MSE of the PCM scheme applied to its \hat{e}_{bi} .

Post-quantization coding of the approximation errors

The number of bits required to encode the approximation errors after the quantization stage can be reduced using the inter-subband correlation by techniques similar to the ones used in JPEG. Thus we suggest coding the DC subband using delta modulation and size-value representation of the differences. Huffman codes are used for the sizes combined with VLI (Variable Length Integer) codes for the values. The AC subbands are coded using zigzag scan, run length coding and once again Huffman coding (of size and run-length pairs) along with VLI codes for the values.

2.4 Summary of the stages of the algorithm

- (1) Apply a CCT \mathbf{M} to the RGB color components of the image to obtain the new color components $C1, C2, C3$.
- (2) Apply the DCT block transform to each color component $Ci, i \in \{1, 2, 3\}$.
- (3) Find the expansion coefficients τ_{b1}, τ_{b0} and β_{b1}, β_{b0} for each of the DCT subbands.

- (4) Quantize the expansion coefficients and output them as part of the compressed image data. Then reconstruct them to obtain $\hat{\tau}_{b1}, \hat{\tau}_{b0}$ and $\hat{\beta}_{b1}, \hat{\beta}_{b0}$.
- (5) Find the approximation errors \hat{e}_{b2} and \hat{e}_{b3} according to (19), and calculate their variances.
- (6) Calculate the optimal rates according to (6) substituting there the selected CCT matrix \mathbf{M} and the variances of the approximation errors. Use the algorithm to find the active subbands according to Subsection 1.2.
- (7) Quantize the approximation errors using uniform quantizers with PCM steps determined according to Subsection 1.3.
- (8) Use post-quantization coding similar to the one used in JPEG. Adaptive Huffman codes are employed in the entropy coding and are sent with the image data. This stage is of course lossless and does not affect the image distortion.

This algorithm uses 2 coefficients for C2 and 2 coefficients for C3, thus we will refer to it as CBA-2-2.

3 Enhanced CBA algorithm

Examining the approximation errors \hat{e}_{bi} coded for the same subband b of C2 and C3, significant correlations can still be noted. This implies that, for example, \hat{e}_{b2} can be coded 'as is' and \hat{e}_{b3} can be expanded using \hat{e}_{b2} . For simplicity, linear approximation can once again be used in this second stage expansion. Denoting the new expansion coefficients δ_{b1} and δ_{b0} , we can easily derive the optimal values for these coefficients

$$\delta_{b1} = \frac{cov(\hat{e}_{b2}, \hat{e}_{b3})}{var(\hat{e}_{b2})}, \quad \delta_{b0} = E(\hat{e}_{b3}) - \frac{cov(\hat{e}_{b2}, \hat{e}_{b3})}{var(\hat{e}_{b2})} \cdot E(\hat{e}_{b2}), \quad (20)$$

where \hat{e}_{b3} is approximated by $\delta_{b1} \cdot \hat{e}_{b2} + \delta_{b0}$. If we neglect the PCM errors in the first stage expansion coefficients, we can write:

$$\begin{aligned} \delta_{b1} &= \frac{cov(y_{b2} - \tau_{b1} \cdot y_{b1} - \tau_{b0}, y_{b3} - \beta_{b1} \cdot y_{b1} - \beta_{b0})}{var(y_{b2} - \tau_{b1} \cdot y_{b1} - \tau_{b0})} \\ &= \frac{var(y_{b1}) \cdot cov(y_{b2}, y_{b3}) - cov(y_{b1}, y_{b2}) \cdot cov(y_{b1}, y_{b3})}{var(y_{b1}) \cdot var(y_{b2}) \cdot (1 - \rho_{b12}^2)}. \end{aligned} \quad (21)$$

Then the theoretical MSE of this approximation for C3 becomes:

$$d_{b3} = var(y_{b3}) \left(\frac{1 - \rho_{b12}^2 - \rho_{b13}^2 - \rho_{b23}^2 + 2 \cdot \rho_{b12} \cdot \rho_{b13} \cdot \rho_{b23}}{1 - \rho_{b12}^2} \right), \quad (22)$$

which when compared to (17) is smaller by a factor of $var(y_{b3}) \frac{(\rho_{b23} - \rho_{b12}\rho_{b13})^2}{1 - \rho_{b12}^2}$ or by a relative portion of $\frac{(\rho_{b23} - \rho_{b12}\rho_{b13})^2}{(1 - \rho_{b12}^2)(1 - \rho_{b13}^2)}$. Note that ρ_{b23} is defined similarly to ρ_{b12} or ρ_{b13} as the inter-color correlation of C2 and C3 in subband b . There is a more efficient way to achieve the same MSE distortion for C3 in one stage approximation. While C2 is still approximated using C1, we suggest that C3 is expanded using C1 and C2 in each subband, so that \hat{y}_{b3} of (10) is replaced by:

$$\hat{y}_{b3} = \beta_{b2} \cdot y_{b2} + \beta_{b1} \cdot y_{b1} + \beta_{b0}. \quad (23)$$

This expansion requires only three coefficients instead of four in the two stage approximation and the expressions for the optimal coefficients in LS sense become:

$$\begin{aligned} \beta_{b2} &= \frac{\rho_{b23} - \rho_{b12} \cdot \rho_{b13}}{(1 - \rho_{b12}^2)} \cdot \sqrt{\frac{var(y_{b3})}{var(y_{b2})}} \\ \beta_{b1} &= \frac{\rho_{b13} - \rho_{b12} \cdot \rho_{b23}}{(1 - \rho_{b12}^2)} \cdot \sqrt{\frac{var(y_{b3})}{var(y_{b1})}} \\ \beta_{b0} &= E(y_{b3}) - \beta_{b2} \cdot E(y_{b2}) - \beta_{b1} \cdot E(y_{b1}). \end{aligned} \quad (24)$$

The variance of the approximation error of subband b of C3 in this expansion is given by the expression of (22), similar to the relation between Equations (17) and (18). As a result, we can write:

$$\begin{aligned} var(e_{b3}) &= var(y_{b3} - \hat{y}_{b3}) \\ &= var(y_{b3}) \left(\frac{1 - \rho_{b12}^2 - \rho_{b13}^2 - \rho_{b23}^2 + 2 \cdot \rho_{b12} \cdot \rho_{b13} \cdot \rho_{b23}}{1 - \rho_{b12}^2} \right). \end{aligned} \quad (25)$$

Practically, the decoder will not have the original C2 component, but the reconstructed one. Thus the reconstructed C2 component should be used in the calculation of the coefficients in (24). Note that the treatment of C2 remains the same as in Section 2.

The stages of the enhanced CBA algorithm become:

- (1) Apply a CCT \mathbf{M} to the RGB color components of the image to obtain the new color components $C1, C2, C3$.
- (2) Apply the DCT block transform to each color component $Ci, i \in \{1, 2, 3\}$.
- (3) Find the expansion coefficients τ_{b1}, τ_{b0} and $\beta_{b2}, \beta_{b1}, \beta_{b0}$ for each of the DCT subbands. Use the original color components in this stage.
- (4) Quantize the expansion coefficients. Then reconstruct them to obtain $\hat{\tau}_{b1}, \hat{\tau}_{b0}$ and $\hat{\beta}_{b2}, \hat{\beta}_{b1}, \hat{\beta}_{b0}$.
- (5) Find the approximation errors:

$$\begin{aligned} \hat{e}_{b2} &\triangleq y_{b2} - \hat{\tau}_{b1} \cdot y_{b1} - \hat{\tau}_{b0} \\ \hat{e}_{b3} &\triangleq y_{b3} - \hat{\beta}_{b2} \cdot y_{b2} - \hat{\beta}_{b1} \cdot y_{b1} - \hat{\beta}_{b0}, \end{aligned}$$

and calculate their variances.

- (6) Calculate the optimal rates according to (6) substituting there the selected CCT matrix \mathbf{M} and the variances of the approximation errors. Use the algorithm to find the active subbands according to Subsection 1.2.
- (7) Quantize the approximation errors of C2 using uniform quantizers with PCM steps determined according to Subsection 1.3. Then reconstruct C2 to be used at the next stage.
- (8) Find the new expansion coefficients $\beta_{b2}, \beta_{b1}, \beta_{b0}$ for C3 using C1 and the reconstructed C2.
- (9) Quantize the new C3 coefficients and reconstruct them. Output the quantized coefficients for C2 and C3.
- (10) Find the new approximation errors \hat{e}_{b3} similar to Step 5.
- (11) Apply the PCM scheme to the new approximation errors of C3 similar to Step 7 for C2.
- (12) Use post-quantization coding similar to the one used in JPEG both for C2 and C3.

Note that the first two stages and the last stage are the same as for the simpler algorithm of Section 2. The enhanced algorithm uses 2 coefficients for C2 and 3 coefficients for C3, thus it will be referred here as CBA-2-3.

4 The optimal CCT transform

Considering the subband coder, described here in the beginning of Section 1.1, the target function, minimized by the optimal CCT was found to be [3]:

$$f(\mathbf{M}) = \prod_{k=1}^3 \left((\mathbf{M}\mathbf{M}^T)^{-1} \right)_{kk} \prod_{b=0}^{B-1} (\sigma_{bk}^2)^{n_b}. \quad (26)$$

The same target function can be used for the CBA algorithms when the approximation error variances are substituted for σ_{bk}^2 . These variances can be expressed by the variances of the subbands of C2 and C3 according to Equation (18) for CBA-2-2 and according to Equations (18) and (25) for CBA-2-3. To express these variances through the image data, we define the subband b covariance matrix $\mathbf{\Lambda}_b$ in the RGB domain:

$$\mathbf{\Lambda}_b \triangleq E \left[\left(\mathbf{Y}_b - \mu_{\mathbf{Y}_b} \right) \left(\mathbf{Y}_b - \mu_{\mathbf{Y}_b} \right)^T \right] \quad \mu_{\mathbf{Y}_b} \triangleq E [\mathbf{Y}_b], \quad (27)$$

where $\mathbf{Y}_b \triangleq [y_{bR} \ y_{bG} \ y_{bB}]^T$ is a vector of the R, G, B DCT coefficients for subband b . Now we can write

$$var(y_{bi}) = \mathbf{m}_i \mathbf{\Lambda}_b \mathbf{m}_i^T \quad (28)$$

and

$$\rho_{bij} = \frac{\mathbf{m}_i \Lambda_b \mathbf{m}_j^T}{\sqrt{(\mathbf{m}_i \Lambda_b \mathbf{m}_i^T)(\mathbf{m}_j \Lambda_b \mathbf{m}_j^T)}}, \quad i \neq j \quad (29)$$

where \mathbf{m}_i stands for row i of \mathbf{M} . Using these expressions, the error variances σ_{bk}^2 can be written as:

$$\sigma_{bk}^2 = \mathbf{m}_k \Lambda_b \mathbf{m}_k^T - \frac{(\mathbf{m}_1 \Lambda_b \mathbf{m}_k^T)^2}{\mathbf{m}_1 \Lambda_b \mathbf{m}_1^T} \quad (k = 2, 3) \quad (30)$$

for CBA-2-2. Similarly, σ_{bk}^2 for CBA-2-3 can be derived. We consider a constant C1 component chosen to be Y of the YUV color space and not compressed. Thus, only the CCT matrix rows corresponding to C2 and C3 are optimized and the CCT target function becomes:

$$f(\mathbf{M}) = \prod_{k=2}^3 \left((\mathbf{M} \mathbf{M}^T)^{-1} \right)_{kk} \prod_{b=0}^{B-1} (\sigma_{bk}^2)^{n_b}. \quad (31)$$

The optimal CCT, i.e., the one minimizing $f(\mathbf{M})$ will be used for the CBA algorithms.

5 Down-sampling the approximation errors and Laplacian rates

5.1 Down-sampling the approximation errors

In JPEG [20] the YUV color components transform is employed and the chrominance components U and V are sometimes down-sampled to provide for less MSE distortion for the same image rate. We propose the same procedure in the case of the approximation errors of the CBA algorithms. However, the down-sampling is to be performed in the image domain, thus the following changes in the algorithms of the previous sections are performed:

- The optimal rates are calculated according to (9) instead of (6).
- Prior to quantization the errors are transformed to image domain by inverse DCT, down-sampled there, for example, by a factor of 2 in each direction and then transformed back to DCT domain.

The performance of the CBA algorithms with and without down-sampling is shown in Tables 1 and 2. The PSPNR (Peak Signal to Perceptible Noise Ratio) here is a subjective distortion measure defined similar to the definition of the PSNR (Peak Signal to Noise Ratio). It is calculated according to:

$$PSPNR \triangleq 10 \log_{10} \frac{255^2}{WMSE}, \quad (32)$$








	Image	PSNR [dB]		PSPNR [dB]		Rate [bpp]
		CBA-2-2 DS	CBA-2-2	CBA-2-2 DS	CBA-2-2	
	Lena	30.03	27.23	41.69	38.97	0.038
	Baboon	30.03	25.75	44.09	38.53	0.075
	Peppers	29.97	28.19	40.63	39.24	0.101
	Tree	29.98	28.62	44.34	42.63	0.081
	House	30.03	28.84	46.59	45.20	0.083
	Jelly Beans	30.00	27.75	45.10	42.88	0.085
	Fruit	29.99	26.62	41.61	37.54	0.057
	Mean	30.00	27.57	43.44	40.71	

Table 1

PSNR and PSPNR results for CBA-2-2 with down-sampling (DS) vs. CBA-2-2 without down-sampling at the same compression rate. The rate is calculated for the C2 and C3 components only.

where $WMSE$ (Weighted Mean Square Error) for each color component is calculated similarly to the MSE of (3) as:

$$WMSE = \sum_{b=0}^{B-1} \eta_b W_b G_b d_b. \quad (33)$$

Here d_b denotes the MSE of subband b , G_b is its energy gain, η_b is its sample rate and W_b is its visual perception weight. Our choice of the WMSE is according to the JPEG2000 algorithm [19]. Also we consider 256x256 size images displayed on a screen as 12cm × 12cm size images.

It can be concluded from the tables that down-sampling improves the performance of the CBA-2-2 algorithm by 2.43dB PSNR and 2.73dB PSPNR on average, while the performance gain of CBA-2-3 is even greater: 3.05dB PSNR and 3.22dB PSPNR on average.





	Image	PSNR [dB]		PSPNR [dB]		Rate [bpp]
		CBA-2-3 DS	CBA-2-3	CBA-2-3 DS	CBA-2-2	
	Lena	29.95	27.33	41.83	39.12	0.039
	Baboon	29.99	25.39	43.89	38.30	0.075
	Peppers	29.97	28.18	40.86	39.66	0.105
	Tree	29.96	28.33	44.18	42.24	0.078
	House	30.04	27.44	46.10	43.30	0.063
	Jelly Beans	30.03	27.20	45.12	43.01	0.084
	Fruit	29.97	24.74	42.02	35.80	0.062
	Mean	29.99	26.94	43.43	40.21	

Table 2

PSNR and PSPNR results for CBA-2-3 with down-sampling (DS) vs. CBA-2-3 without down-sampling at the same compression rate. The rate is calculated for the C2 and C3 components only.

5.2 Laplacian rates

The distribution of the coefficients of the block DCT was analyzed in [13]. It has been found that this distribution can be modelled as Laplacian. Employing this probability model, we can approximately calculate the subband rates without the use of histograms. Given a subband b of color component i having a variance σ_{bi}^2 and quantized with a step Δ_{bi} , the rate of the subband is approximated by [2]:

$$\begin{aligned}
 R_{bi} = & - \left(1 - e^{-0.5\mu_{bi}\Delta_{bi}}\right) \log_2 \left(1 - e^{-0.5\mu_{bi}\Delta_{bi}}\right) - e^{-0.5\mu_{bi}\Delta_{bi}} (\log_2 k_{bi} - 1) \\
 & + \frac{\mu_{bi}\Delta_{bi}}{k_{bi}} \log_2(e),
 \end{aligned} \tag{34}$$

where

$$k_{bi} \triangleq e^{0.5\mu_{bi}\Delta_{bi}} - e^{-0.5\mu_{bi}\Delta_{bi}}, \quad \mu_{bi} \triangleq \sqrt{\frac{2}{\sigma_{bi}^2}}. \quad (35)$$

The benefit of using Equation (34) for the rates calculation is the reduced complexity of the algorithms [2]. As for the performance, it is also increased on average as seen from Table 3 by about 0.5-0.6dB PSNR and 0.4-0.6dB PSPNR.

Mean PSNR [dB]		Mean PSPNR [dB]	
CBA-2-2 LR DS	CBA-2-2 DS	CBA-2-2 LR DS	CBA-2-2 DS
30.02	29.54	43.25	42.89
CBA-2-3 LR DS	CBA-2-3 DS	CBA-2-3 LR DS	CBA-2-3 DS
30.00	29.43	43.81	43.23

Table 3

Mean PSNR and PSPNR results for the images of Tables 1 and 2 for CBA-2-2 and CBA-2-3 with Laplacian rates (LR) and down-sampling (DS) compared to the same algorithms with real rates and down-sampling at the same compression rate. The rate is calculated for the C2 and C3 components only.

6 The zero order coefficients

In Stage 4 of the CBA-2-2 algorithm (Subsection 2.4) we have proposed transmitting both the first order τ_{b1}, β_{b1} coefficients and the zero order τ_{b0}, β_{b0} coefficients. However, as we saw in the discussion following Equation (12), it is the first order coefficients that minimize the variances of the approximation errors, thus allowing better compression of the errors. The zero order coefficients on the other hand only bring the mean value of the errors to zero. If we consider a non-active subband, the effect of this is that minimal variance of the LS approximation error is equivalent to minimal MSE distortion for the subband (disregarding the influence of the PCM errors of the coefficients) and thus sending the zero order coefficients may be useful. On the other hand, the non-active subbands contain a small portion of the energy of the image and their contribution to the total MSE distortion is not significant. For an active subband it is the error variance that is important and resetting the error's mean may only allow better performance in the post-quantization stage of Subsection 2.3.

Thus we propose another version of the algorithm of Section 2 that uses only the τ_{b1}, β_{b1} coefficients found according to Equations (13) and (14). A comparison of this algorithm denoted CBA-1-1 and the CBA-2-2 algorithm is shown in Table 4 for various images. Note that both down-sampling and Laplacian rates have been used here for both algorithms. The conclusion from Table 4






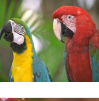

	Image	PSNR [dB]		PSPNR [dB]		Rate [bpp]
		CBA-1-1	CBA-2-2	CBA-1-1	CBA-2-2	
	Girl	30.03	29.78	44.77	44.37	0.061
	Hats	30.02	28.68	41.65	41.00	0.040
	Fruits	30.00	29.86	42.68	42.50	0.091
	Frog	30.02	29.47	40.14	39.17	0.051
	Landscape	30.03	29.17	41.26	40.22	0.025
	Parrots	30.05	29.55	42.21	41.61	0.047
	Monarch	29.96	29.85	44.33	44.14	0.076
	Mean	30.01	29.48	42.43	41.86	

Table 4

PSNR and PSPNR results for CBA-1-1 vs. CBA-2-2 at the same compression rate. Both algorithms use down-sampling and Laplacian rates. The rate is calculated for the C2 and C3 components only.

is that the CBA-1-1 algorithm is superior to CBA-2-2 with an average performance gain of 0.53dB PSNR and 0.57dB PSPNR.

A similar version of the CBA-2-3 algorithm can be introduced using only the τ_{b1} coefficients for C2 and β_{b1}, β_{b2} for C3. We denote this version as CBA-1-2 as it uses one expansion coefficient for C2 and two for C3. A comparison of this algorithm with the original CBA-2-3 (using down-sampling and Laplacian rates for both algorithms) is given in Table 5. It can be seen that once again CBA-1-2 is superior, with gains of 0.48dB PSNR and 0.64dB PSPNR.

7 Simulation and comparison

In this section we compare the CBA algorithms to the popular JPEG algorithm as a representative of the de-correlation approach. First we consider the






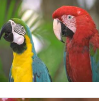

	Image	PSNR [dB]		PSPNR [dB]		Rate [bpp]
		CBA-1-2	CBA-2-3	CBA-1-2	CBA-2-3	
	Girl	29.97	29.86	45.02	44.67	0.065
	Hats	29.96	28.06	42.29	40.32	0.041
	Fruits	29.95	29.89	42.99	42.65	0.095
	Frog	29.96	29.63	39.98	39.46	0.055
	Landscape	30.05	29.82	41.31	40.64	0.025
	Parrots	30.01	29.43	41.86	41.40	0.047
	Monarch	30.01	29.86	44.34	44.12	0.077
	Mean	29.99	29.51	42.54	41.90	

Table 5

PSNR and PSPNR results for CBA-1-2 vs. CBA-2-3 at the same compression rate. Both algorithms use down-sampling and Laplacian rates. The rate is calculated for the C2 and C3 components only.

case of no down-sampling (DS) of the color components. A comparison of the basic CBA-2-2, CBA-2-3 algorithms and JPEG is shown in Fig. 1. Better visual quality can be observed for the images produced by the CBA algorithms when compared to JPEG images. Also quantitative gains of more than 2dB and up to almost 3dB can be measured both in the PSNR and the PSPNR for the CBA-2-2 algorithm [5]. The performance is lower for the CBA-2-3 algorithm, but still much higher than JPEG's.

When employing down-sampling of the chrominance information in JPEG and of the subordinate colors in the CBA algorithms, smaller gains in the PSNR and PSPNR should be expected. Since this is likely to be the more practical case today, a comparison of the CBA algorithms and JPEG with down-sampling is of interest. Such a comparison is provided in Fig. 2. We consider the best algorithms according to the previous sections: CBA-1-1 and CBA-1-2. It can be seen that JPEG introduces color artifacts, especially visible in the parts marked in red. Those artifacts are less pronounced in the CBA

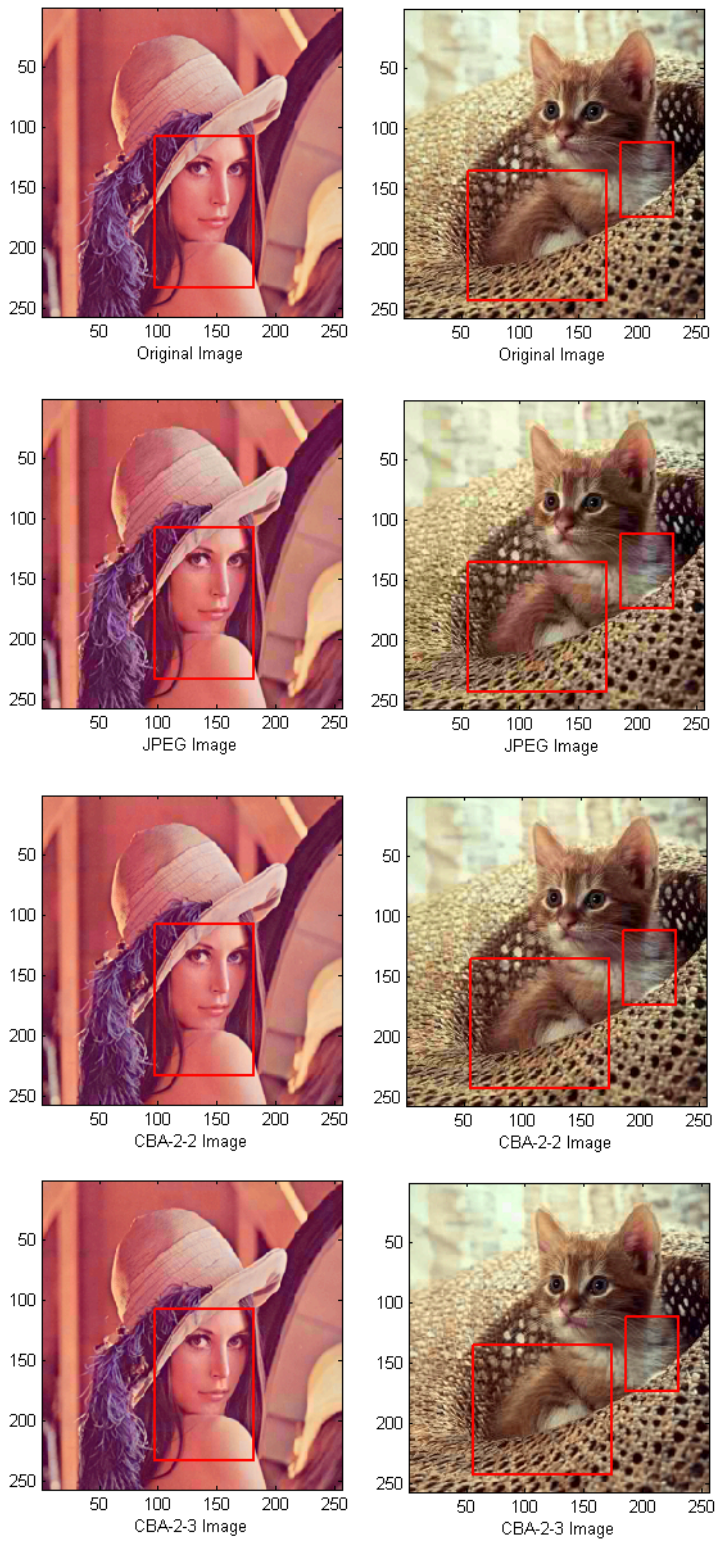


Fig. 1. Lena and Cat images - from top to bottom: original, compressed by JPEG and compressed by the CBA-2-2 and CBA-2-3 algorithms (without DS for all). PSNR for the Lena image: 30.38 (JPEG), 32.78 (CBA-2-3) and 33.00 (CBA-2-2). PSPNR: 43.95 (JPEG), 45.89 (CBA-2-3) and 46.05 (CBA-2-2) at 0.109bpp. PSNR for the Cat image: 32.18dB for JPEG and 35.02dB for CBA-2-3 and CBA-2-2. PSPNR: 44.15dB (JPEG), 46.12dB (CBA-2-3) and 46.97dB (CBA-2-2) at 0.066bpp.

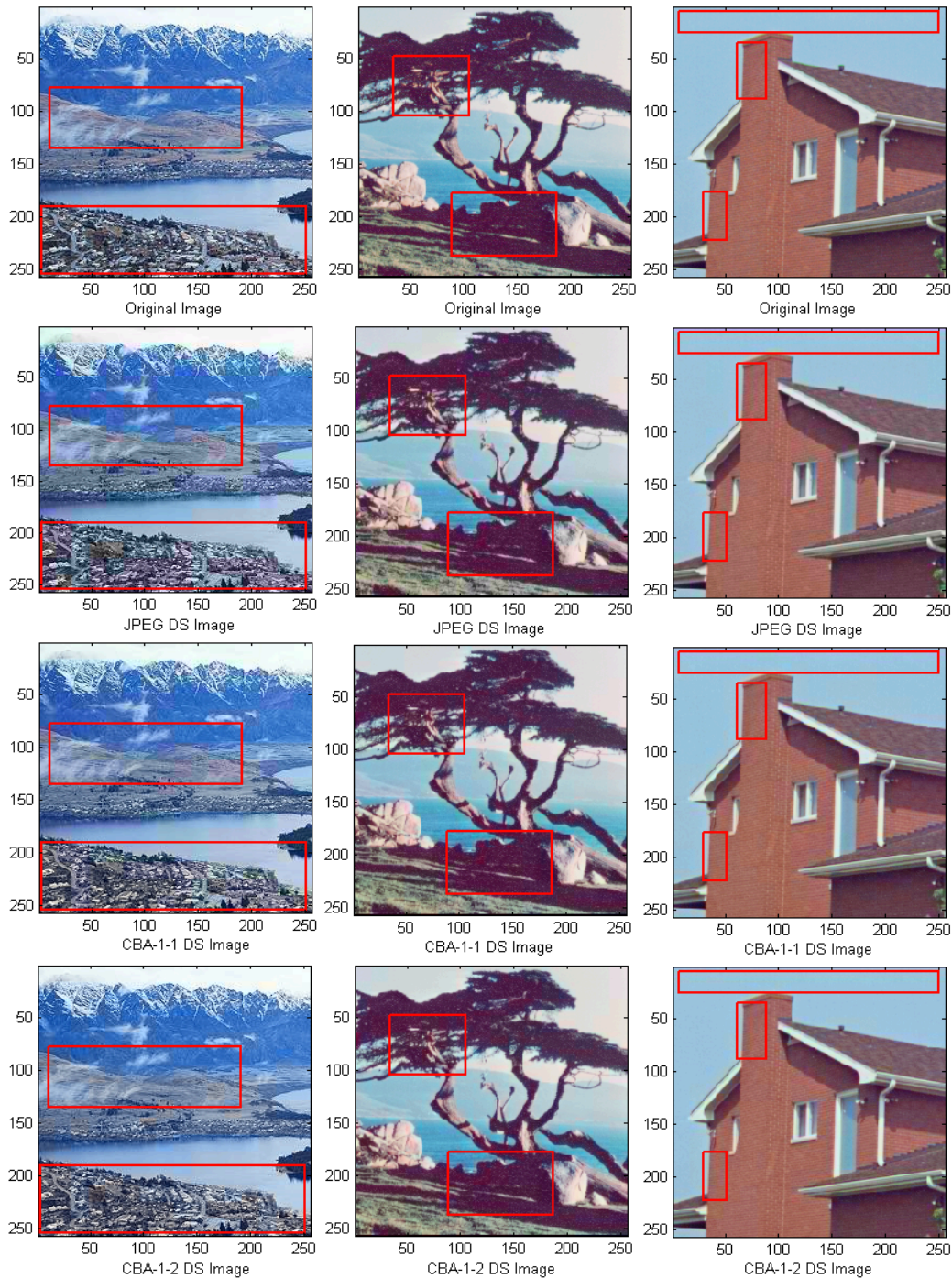


Fig. 2. Landscape, Tree and House images - from top to bottom: original and 3 compressed versions: by JPEG, by CBA-1-1 and by CBA-1-2 (with DS for all). PSNR for the Landscape image: 32.24 (CBA-1-1), 33.28 (CBA-1-2) and 30.17 (JPEG). PSPNR: 43.08 (CBA-1-1), 44.31 (CBA-1-2) and 40.87 (JPEG) at 0.028bpp. PSNR for the Tree image: 30.04 (CBA-1-1), 29.96 (CBA-1-2) and 28.85 (JPEG). PSPNR: 44.25 (CBA-1-1), 44.08 (CBA-1-2) and 43.38 (JPEG) at 0.067bpp. PSNR for the House image: 31.60 (CBA-1-1), 31.52 (CBA-1-2) and 30.39 (JPEG). PSPNR: 47.52 (CBA-1-1), 47.55 (CBA-1-2) and 47.28 (JPEG) at 0.078bpp.

algorithms. Also while for the Landscape image CBA-1-2 has definitely best performance and for the Tree image CBA-1-1 is slightly better, for the House image both CBA algorithms are about the same.

8 Summary

A new approach to color image compression has been introduced. The approach is based on exploiting the inter-color correlations between the color primaries instead of transforming them into a de-correlated color space. Based on this approach, two new compression algorithms have been introduced, employing the block DCT transform. Both algorithms use first-order linear approximation of two of the color components (C2 and C3) in each DCT subband based to the third color component (C1). However, our second algorithm, denoted CBA-2-3, is more complex since it approximates one of the dependent colors relative to the base as well as the second dependent color. It has been shown how these algorithms can be optimized in the choice of the color components transform and the subband rates allocation using the theory presented in [4]. This theory is based on a Rate-Distortion model for subband transform coders as well as common constraints [15]. Furthermore, the algorithms' performance can be significantly improved using down-sampling of the subordinate colors (C2 and C3) and using a Laplacian model for the DCT coefficients. This model also allows for the reduction of complexity of the algorithms. Additional improvement is possible by using only first order expansion coefficients, avoiding transmission of the zero order coefficients.

Simulation results have been provided, demonstrating the advantage of the proposed techniques. In Section 7 the CBA algorithms have been compared to JPEG, demonstrating superior performance both visually and quantitatively. Our conclusion is that the new CBA approach could be superior to the common approach of de-correlation.

Acknowledgement

This research was supported in part by the HASSIP Research Program HPRN-CT-2002-00285 of the European Commission, and by the Ollendorff Minerva Center. Minerva is funded through the BMBF.

References

- [1] Gershikov E., Porat M., A Rate-Distortion Approach to Optimal Color Image Compression, *14th European Signal Processing Conference (EUSIPCO 2006)*, Florence, Italy, 2006.
- [2] Gershikov E., Porat M., An Optimization Based Approach to Color Image Compression Using a Rate-Distortion Model, *The Sixth IASTED International Conference on Modeling, Simulation and Optimization (MSO)*, 2006.
- [3] Gershikov E., Porat M., Data Compression of Color Images using a Probabilistic Linear Transform Approach, *The Sixth International Conference on Numerical Methods and Applications (NM&A)*, 2006.
- [4] Gershikov E. and Porat M., On Color Transforms and Bit Allocation for Optimal Subband Image Compression, in press *Signal Processing: Image Communication*.
- [5] Gershikov E., Lavi-Burlak E. and Porat M., On a Rate-Distortion Model for Color Images using a Correlation-Based Approach, *the 24th IEEE Israeli Conference*, Eilat, 2006.
- [6] Gershikov E. and Porat M., Does Decorrelation Really Improve Color Image Compression?, *the International Conference on Systems Theory and Scientific Computation (ISTASC05)*, Malta, 2005.
- [7] Gersho A. and Gray R. M., *Vector Quantization and Signal Compression*, Boston, MA: Kluwer, Ch. 2, 1992.
- [8] Goffman-Vinopal L. and Porat M., Color image compression using inter-color correlation, *IEEE International Conference on Image Processing*, Vol.2, pp. II-353 - II-356, 2002.
- [9] Goffman-Vinopal L., *The Effect of Intercolor Correlation on Color Image Compression*, Graduate School Thesis, Technion, 2001.
- [10] JPEG 2000 Part I: Final Draft International Standard (ISO/IECFDIS15444-1), ISO/IEC JTC1/SC29/WG1 N1855, Aug. 2000.
- [11] Kotera H. and Kanamori K., A Novel Coding Algorithm for Representing Full Color Images by a Single Color Image, *J. Imaging Technology*, Vol. 16, pp. 142-152, 1990.
- [12] Kouassi R.K., Gouton P. and Paindavoine M., Approximation of the Karhunen-Loève transformation and its application to colour images, *Signal Processing: Image Communication*, Vol. 16, pp. 541-551, 2001.
- [13] Lam E. Y. and Goodman J. W., A mathematical analysis of the DCT coefficient distributions for images, *IEEE Trans. on Image Processing*, Vol. 9, No. 10, pp. 1661-1666, 2000.

- [14] Limb J. O. and Rubinstein C.B., Statistical Dependence Between Components of A Differentially Quantized Color Signal, *IEEE Trans. on Communications*, Vol. Com-20, pp. 890-899, Oct. 1971.
- [15] Porat M. and Shachor G., Signal Representation in the combined Phase - Spatial space: Reconstruction and Criteria for Uniqueness, *IEEE Trans. on Signal Processing*, vol. 47, No. 6, pp. 1701-1707, 1999.
- [16] Rabbani M. and Joshi R., An overview of the JPEG2000 still image compression standard, *Signal Processing: Image Communication*, Vol. 17, No. 1, pp 3-48, 2002.
- [17] Rao K. R. and Yip P., Discrete cosine transform: algorithms, advantages, applications, Academic Press, 1990.
- [18] Roterman Y. and Porat M., Color Image Coding using Regional Correlation of Primary Colors", in press *Elsevier Image and Vision Computing*, 2006.
- [19] Taubman D. S. and Marcellin M. W., JPEG2000: image compression, fundamentals, standards and practice, Kluwer Academic Publishers, 2002.
- [20] Wallace G. K., The JPEG Still Picture Compression Standard, *IEEE Transactions on Consumer Electronics* , Vol. 38, pp. xviii-xxxiv, 1992.
- [21] Wolf S. G., Ginosar R. and Zeevi Y. Y., Spatio-chromatic Model for Colour Image Processing, *IEEE Proc. of the IAPR*, Vol. 1, pp. 599-601, 1994.
- [22] Yamaguchi H., Efficient Encoding of Colored Pictures in R, G, B Components, *Trans. on Communications*, Vol. 32, pp. 1201-1209, Nov. 1984.